5-2018

The role of ferric reduction oxidases in plant anti-herbivore defense.

Virginia C. Nunamaker
University of Louisville

The Role of Ferric Reduction Oxidases in Plant Anti-Herbivore Defense

By

Virginia Nunamaker

Submitted in partial fulfillment of the requirements for Graduation *summa cum laude*

University of Louisville

May 2018

Table of Contents

Abstract

Iron is an essential element required for plants to carry out metabolic functions such as photosynthesis, heme biosynthesis, and chlorophyll biosynthesis. Within *Arabidopsis thaliana*, eight ferric reduction oxidase (FRO) genes function in iron uptake and homeostasis with tissue specific expression. However, little else is known regarding the biological role of FROs. Recent studies identify the FRO gene family as particularly responsive to the green leaf plant derived volatile (GLV) *cis*-3-hexenyl acetate (z3HAC). Since z3HAC acts as a wound signal and cues unaffected parts of the plant to prime defenses prior to herbivory, an increase in FRO activity in response to volatile perception may suggest that these metalloreductases play a role in plant anti-herbivore defense. The objective of this study was to measure transcriptional responses of FROs to herbivore oral secretions (OS) and plant-derived volatile cues. Results of this study show FROs differentially increase expression levels in response to herbivory and volatile exposure. Specifically, z3HAC alone induced expression of FRO3, FRO4, and FRO6. In addition, a number of FROs were primed by the combination of z3HAC and *Spodoptera exigua* OS including FRO4 and FRO7, suggesting iron homeostasis in leaves may be important in plant anti-herbivore defense. Future work needs to identify a mechanism linking FROs and herbivory.

Background

Iron (Fe) is a required element for plants to carry out essential metabolic processes including chlorophyll biosynthesis, photosynthesis, and nucleotide synthesis (Guerinot et al. 2007). In addition, iron in the form of heme or iron-sulfur is an essential component of numerous proteins and enzymes (Marschnew 1995). While highly abundant in soil, iron's low solubility in aerobic environments at biological pH restricts cellular accumulation thus limiting plant growth and development. Identified by chlorotic or yellowed leaves, iron deficiency can cause yield reduction and sometimes total crop failure (Guerinot et al 1994). Higher level plants such as dicots, nongraminaceous monocots, and yeast have evolved mechanisms to increase the availability of iron for absorption via acidification of the rhizosphere, reduction of Fe(III) to Fe(II), and then transport of Fe(II) across the cell membrane (Dancis et al. 1992). This reduction of Fe(III) to Fe(II) requires an inducible ferric reduction oxidase (FRO) on the plasma membrane of root epidermal cells. The reduction takes place on the root-rhizosphere surface and a ferrous iron transporter, IRT1, subsequently transports the reduced ferrous iron across the plasma membrane (Jain et al. 1992)

In *Arabidopsis thaliana*, eight genes have been classified in the FRO metalloreductase family due to conserved motifs based on FRO2 found in the roots of *A. thaliana* (Figure 1a; TAIR 2013). These metalloreductases function in iron acquisition and homeostasis of *A. thaliana* with tissue-specific expression (Wu et al. 2005). Expression profiles indicate FRO2 and FRO3 as major iron reductases expressed in the roots of *A. thaliana* (Jain et al. 2014). Expression of both FRO2 and FRO3 increase under iron deficient conditions. Expression of FRO8 has also been identified in roots under iron-deficient conditions, however FRO8 is expressed constitutively at relatively high levels in shoots and leaf veins (Jain et al. 2014; Wu et al. 2005).

FRO4 has also been found expressed in roots and shoots of *A.thaliana*, although in relatively low levels. Expression of FRO5 and FRO6 is transcribed constitutively in shoots and flowers regardless of iron levels, while FRO7 is expressed mainly in trichrome and cotyledons (Wu et al. 2005). Regulation of FRO6 expression has also been suggested as specifically light dependent (Feng et al. 2006). These tissue-specific expressions suggest FRO2 and FRO3 function as the main reductases involved in root iron acquisition, while shoot tissues utilize FRO4, FRO5, FRO6, FRO7, and FRO8 for iron homeostasis (Wu et al. 2005). More recent studies further elucidate specific FROs as important to subcellular compartmentalization of iron where FRO7 contributes to the delivery of iron to chloroplasts (Jain et. al 2014). Localized to the chloroplasts of young seedlings, FRO7 is required for their efficient photosynthesis and survival under iron-limiting conditions (Jeong et al. 2008). Similarly, FRO8 is localized to and maintains iron homeostasis in the mitochondria (Jain et al. 2014). The tissue specific expression of FROs indicates an evolution of functional diversification within the gene family resulting in systemic iron acquisition and homeostasis benefits in *A. Thaliana*.

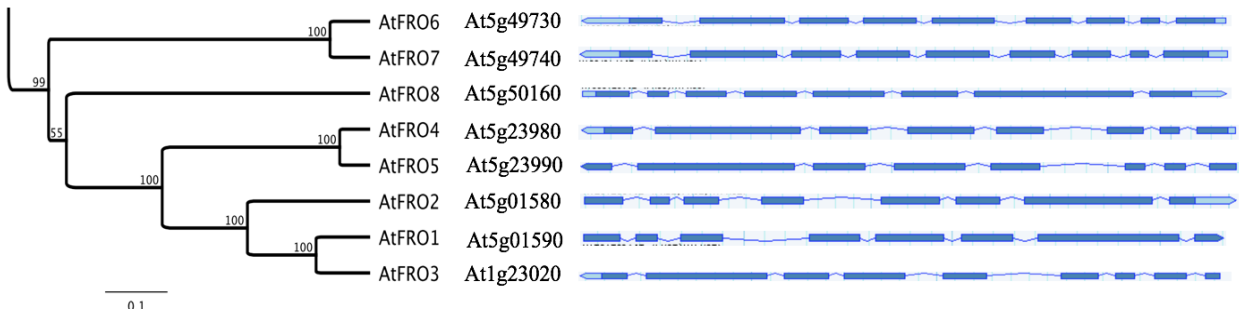

Fig 1a. FRO Phylogeny with locus details corresponding to each FRO's transcribed region in *A. Thaliana* genome, and a Map Detail Image showing the Protein Coding Gene Model for each FRO. This information was generated from consensus sequence alignment found in the genetic and molecular database The Arabidopsis Information Resource (TAIR).

Sequence homology performed online through TAIR identifies respiratory burst oxidase homologs (RBOH), also known as NADPH oxidases (NOXs), as the closest relatives of FROs (Figure 1b; TAIR 2013). Based on domain composition obtained through Gene Structure Display Server, FROs originated from a single common ancestor that contained only a ferric reduction domain. Subsequent gene fusion and duplication events led to FAD and NAD binding domains and the ultimate expansion of the FRO family into Rhodophyta, green algae, and land plants. This ancestral FRO also gave rise to plant NOX genes through fusion and duplication in red or green algae (Chang 2016). Further analysis of intron gains or loss of FROs and NOXs show highly conserved introns and intron phases within subfamilies but vary between them, indicating that a single intron loss or gain could have resulted in the functional diversification and divergence of FRO and NOX gene families (Li et. al 2009: Chang 2016).

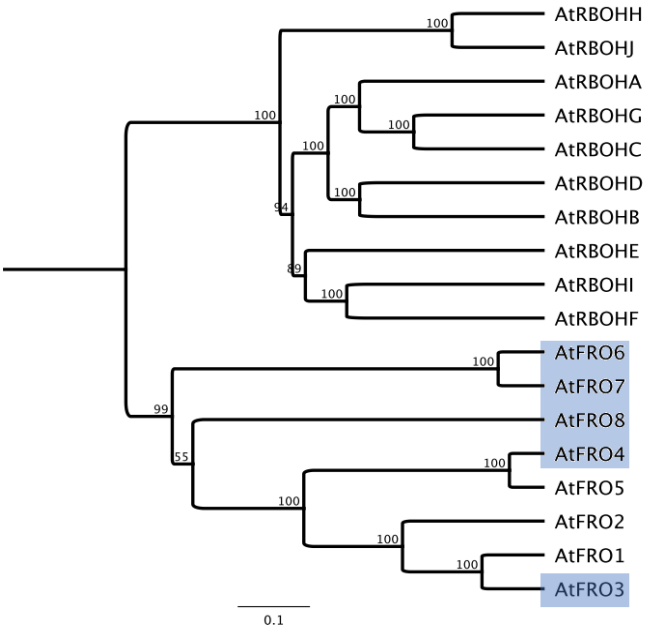

Fig 1b. Phylogenetic tree showing RBOHs as closest relative of FROs. The numbers at each joint represent bootstrap confidence levels. FROs highlighted in blue are FROs expressed in leaf-tissues that will be analyzed in this study.

Whereas FROs known responsibility lies in iron uptake and homeostasis, NOXs are key producers of reactive oxygen species under stress conditions. Being mainly responsible for stress tolerance, NOXs have recently been suggested as required for a rapid defense propagation in *A. thaliana* (Dubiella et. al 2013). Due to the close relationship FROs have to these oxidases involved in stress tolerance, FROs ability to acquire and maintain iron homeostasis could also be essential to a plant's ability to propagate a

rapid defense. For example, the nutritional status of plant's iron can control the outcome of a pathogenic infection with lower pathogenic resistance in iron deficient plants (Kieu et al. 2012). Furthermore, studies involving *A. thaliana* colonization by *Trichoderma* fungi suggest that iron is a critical element in a plant's induced systemic response to a biotic stress resulting in primed chemical defenses in unaffected parts of the plant (Martinez-Medina et al. 2017).

While iron homeostasis has been identified as a critical element in a plant's ability to respond to direct biotic stress, nothing is known regarding FROs activity in response to herbivory and thus the biological role FROs may play in plants anti-herbivore defense. Released upon herbivory, the green leaf plant-derived volatile (GLV) *cis*-3-hexenyl acetate (z3HAC) acts as a wound signal by communicating the presence of a biotic stressor to and within a plant (Frost et al. 2008). Plants recognize and respond to the emission of this herbivore induced plant volatile (HIPV) by priming herbivore defenses prior to herbivory (Frost et al. 2008; War et al. 2011). Defensively, priming is a physiological process by which a plant prepares quicker and more aggressive responses to future stessors such as herbivory (Frost et al. 2008). Previous RNA sequencing work in the Frost Lab at the University of Louisville identifies the FRO gene family as particularly responsive to z3HAC, indicating that FRO activity may be directly responsive to herbivory or the perception thereof. Increased FRO expression in response to herbivory or primed expression in response to HIPV perception suggests a biological role of FROs in plant anti-herbivore defense. Further exploration of the biological functions of FROs in response to herbivory and particularly HIPV perception has the potential to help generate iron efficient crops while controlling the spread of disease or pests.

Research Goals

Initial RNA sequencing shows activation of particular FROs (FRO3, FRO4, FRO6, FRO7, FRO8) at a single time point following GLV exposure. The objective of this study was to further establish FRO involvement in the biological response to herbivory and HIPV perception by measuring transcriptional responses of FROs to a combination of herbivore oral secretions (OS) and volatile exposure. Specifically, this study aims to determine and validate primers for measuring FRO genes and to determine expression patterns for specific FRO family members in *Arabidopsis thaliana* following exposure to z3HAC, herbivore OS, and z3HAC+herbivore OS. Measuring transcriptional activity of FROs in response to OS and plant-derived volatile cues will begin to elucidate FRO response to herbivory and possible involvement in plant anti-herbivore defense.

Materials and Methodology

A. thaliana plants were grown in a growth chamber with a 12:12 light: dark cycle. Plants in the rosette stage were exposed to z3HAC at low concentrations (10 ng/hr) for 24 hours. Subsequently, OS from *Spodoptera exigua*, and *Trichoplusia ni* caterpillars were added to undamaged rosette leaves using a factorial design (control, z3HAC, *S. exigua* OS, z3HAC+ *S. exigua* OS, *T. ni* OS, and z3HAC+ *T. ni* OS). At 1, 6, and 24 hours after OS application rosette leaves were harvested directly into liquid nitrogen and stored at -80˚ C. Individual plants were used as the unit of replication with four plants per treatment per time point, representing 48 individual plants.

Leaf tissue were ground under cryogenic conditions and total RNA was extracted using a modified cetyl trimethylammonium bromide (CTAB) method. This CTAB method took approximately 24 hours and required maintaining RNAse-free conditions at all times (Chang et

Table 1. Solutions included to make 25 ml stock of CTAB extraction buffer. CTAB buffer was brought to final volume with the addition of RNAse free water.

CTAB Extraction Buffer	[Stock]	[Final]	For 25 ml
CTAB	--	2%	0.5g
Polyvinylrrolidone (PVP)	--	2%	0.5g
Tris-HCL (pH 8.0)	1M	100mM	2.5mL
EDTA (pH 8.0)	0.5M	25mM	1.25mL
NaCl	5M	2M	10mL
β-mercaptoethanol (βME)	--	2%	0.5mL

al., 1993). Rosette leaves for each sample were removed from -80˚C storage, ground with mortar/pestle, and approximately 200mg of each ground tissue dispensed into pre-chilled 2µl tubes. Under a chemical hood, 1ml of CTAB extraction buffer was added to the samples and samples were subsequently vortexed to integrate buffer and placed in 65° C bath. A 25 ml stock of CTAB buffer was prepared previous to RNA extraction (Table 1). After sitting for 10 min in a 65° C bath, 100 µl of chloroform was added to each sample and samples were again vortexed for 10-20 seconds. Lime green in color, the solutions were then spun for 10 min at 20,000 × *g* at 4° C. Subsequently, the aqueous layer of each sample was transferred to a new tube already containing 600 µl of chloroform and vortexed. Solutions were then spun again for 10 min at 20,000 × *g* at 4° C. After being spun, the aqueous layer of each sample was again transferred to a tube containing 200 ul of 10M lithium chloride. Samples were gently inverted and precipitated overnight (Chang et al., 1993).

For best extraction results, samples were not left on ice longer than 15 hrs (Frost et al., 2012). Following LiCl precipitation, samples were spun at 20,000 × *g* at 4° C to pellet the RNA. The supernatant waste was decanted into waste container and remaining liquid was removed from the pellet. The pellet was then dissolved in 500 µl RNAse free water, vortexed, and placed

in 65° C bath. Once completely dissolved, 500 µl of chloroform was added to the sample followed by a quick vortex and spin for 3 min at 5000 rpm, room temperature. Subsequently, the aqueous layer was transferred to a new tube containing 0.1vol (50 µl) 3M NaOAc and 2vol (1 ml) of ice-cold EtOH. Samples were gently inverted and precipitated for 20 min at -80˚C. Each sample was again spun for 30 minutes at 20,000 × *g* at 4° C and the supernatant discarded. After air drying the now opaque pellet, the RNA sample was re-suspended in 50 µl of RNAse free water and 1 µl of each sample was run on a nanodrop and gel electrophoresis for quality assessment (Figure 2). Tubulin beta 8 (TUB8), a gene widely expressed in vascular tissues of *A. thaliana* leaves, stems, and flowers was used as a reference gene during gel electrophoresis.

After quality assessment with a ThermoScientific NanoDrop and gel electrophoresis, total RNA was subjected to cDNA synthesis by reverse transcription using Applied Biosystems cDNA Synthesis Kit. cDNA was amplified using quantitative PCR (qPCR) on an Applied Biosystems QuantStudio3. A 25 µl working stock for the qPCR included 9.5 µl of double distilled water, 2 µl of cDNA, .5 µl of forward and reverse RNA primers, and 12.5. µl of a master mix. The master mix includes $MgCl_2$, a buffer, dNTPs, and tag DNA Polymerase. 10 µl of each sample was loaded onto tray with three biological replicates per sample. Each sample was run for three different time points (1hr, 6hr, and 24hr). Including two housekeeping genes TUB8 and Elongation Factor 1 (EF1), 7 samples were run on the qPCR machine each with 35 cycle times

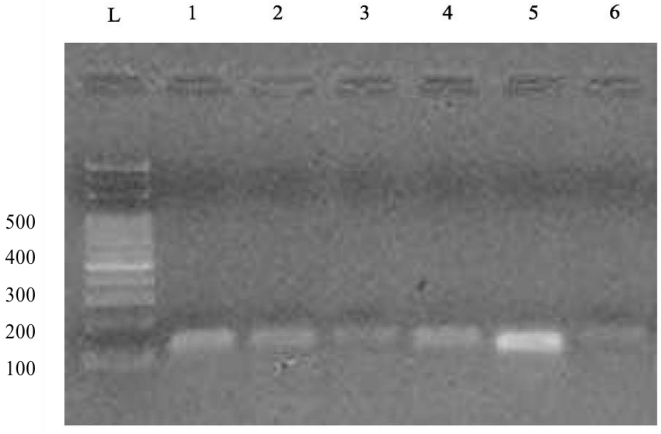

Figure 2. Results of amplifications of fragments of FRO genes expressed in leaf tissue. FRO genes amplified include FRO3 (Lane 1), FRO4 (Lane 2), FRO6 (Lane 3), FRO7 (Lane 4), FRO8 (Lane 5), and reference gene TUB8 (Lane 6). Using Ladder DNA (Lane L) amplicon sizes of all FROs were confirmed at 220 base pairs (bp).

Table 2. A list of FRO Primer sequences. AGI code, expected amplicon size, and reference.

Gene Name	Primer Type	Primer Sequence	Expected Amplicon Size (bp)	AG1 Code	Reference
FRO3	Forward	GACACTCTCTTAGTTGGCGGT	109	At1g23020	Designed by NCBI
FRO3	Reverse	CACTCCGTCGTTCCCTTACC			
FRO4	Forward	GCCCGAGACAACTGATGACCA	199	At5g23980	Designed by NCBI
FRO4	Reverse	TCACAACTCCGAGCCAGAGGA			
FRO6	Forward	TGGAAACAGCTATGGTTGATATG	124	At5g49730	Mukherjee et al. 2006
FRO6	Reverse	TGTCCAATGTAGAAACACCAACA			
FRO7	Forward	CACTCTCTTTGGCCTCACAG	117	At5g49740	Mukherjee et al. 2006
FRO7	Reverse	TTAGTGAAAACCGTCTCTTCC			
FRO8	Forward	GGCGGGAGGAATTGGGATCA	102	At5g50160	Designed by NCBI
FRO8	Reverse	ACCGCAAACACAAGCTGCAC			
TUB8	Forward	ATCCCATTCCCTCGTCTCCA	91	At5g23860	Designed by NCBI
TUB8	Reverse	CAGGGACGGTTAAGGCTCTG			
EF1	Forward	CCAGCTAAGGGTGCCGCCAA	106	At5g60390	Designed by NCBI
EF1	Reverse	TGTGAGAGGTGTGGCAATCGAGA			

(1.5hrs/sample), culminating in a total of 63 samples run on qPCR. Supplementary Figures I-V show amplification plots and melting curves for each 6-hour FRO sample run on qPCR.

Gene specific primers were designed either from literature or using the Primer3 Software Suite through NCBI to amplify in the 3' UTR of each gene (Table 2). Confirmed with gel electrophoresis, each primer pair generated a single amplicon based on a single band PCR product. After sequencing these amplicons to confirm gene specific identification, qPCR analysis was used to determine transcript levels. The relative transcript abundance gene interest equation ($=2^{-\Delta Ct}$) was used to determine target transcript levels normalized to the geometric mean of housekeeping genes Tubulin and EF1.

Results

FRO3 was activated after 24 hours of herbivory and z3HAC+herbivory.

FRO3 did not experience significant upregulation of expression after 1 or 6 hours under any treatment (Figure 3). After 24 hours, the expression level of FRO3 increased under z3HAC+*S. exigua* OS, z3HAC+*T. ni* OS, and z3HAC treatments relative to control expression levels

(Figure 3). 24 hours post z3HAC+*S. exigua* OS application, FRO3 experienced a 1.37-fold change in regulation with higher expression levels relative to control (P=0.005; Figure 3). 24 hours following z3HAC+*T. ni* OS application, FRO3 saw increased expression relative to control (P=0.03; Figure 3). FRO3 had a 1-fold upregulation after 24 hours of z3HAC exposure compared to control levels (P=0.04; Figure 3). No significant priming of FRO3 by z3HAC took place under any treatments at any time points.

FRO4 was activated after 24 hours of z3HAC exposure and z3HAC+*S. exigua* OS. FRO4 was primed by the combination of z3HAC+*S. exigua* OS 24 hours post treatment application.

FRO4 did not experience any increase in expression 1 or 6 hours following any treatment application when compared to control levels (Figure 4). After 24 hours of z3HAC+*S. exigua* OS

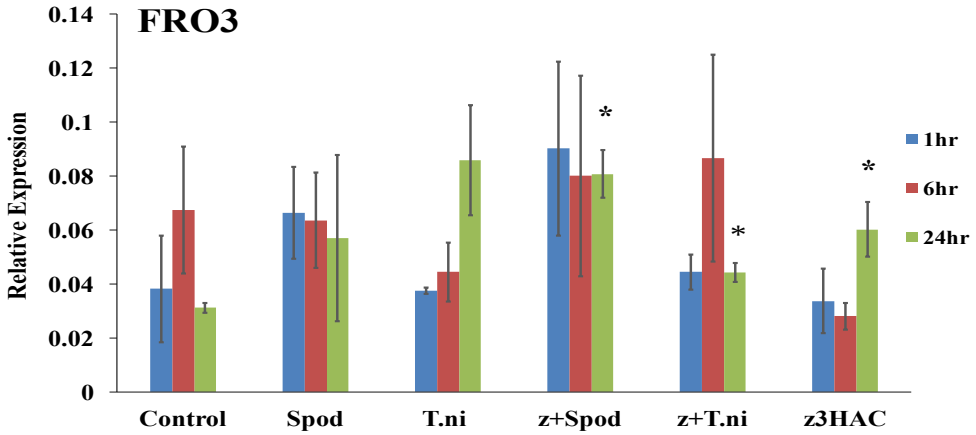

Figure 3. Ferric Reduction Oxidase 3 (FRO3) relative expression levels following exposure to *cis*-3-hexenyl acetate (z3HAC), *Trichoplusia ni* oral secretions (T.ni), *Spodoptera exigua* oral secretions (Spod), *cis*-3-hexenyl acetate with subsequent *Spodoptera exigua* oral secretions (z+Spod), and *cis*-3-hexenyl acetate with subsequent *Trichoplusia ni* oral secretions (z+T.ni) relative to control with no oral secretion application or z3HAC exposure. Expression levels were recorded for each treatment at 1-hour (blue) 6-hour (red) and 24-hour (green) time points post treatment application. An asterisk (*) indicates that expression levels were significantly different than that of control at that time point, as determined by paired t-tests. A number sign (#) indicates significantly increased expression with *cis*-3-hexenyl acetate prior to oral secretions relative to expression under oral secretions alone, as determined by paired t-tests.

exposure, FRO4 had higher expression levels relative to that of the control with a 1.4-fold increase in expression (P=0.02; Figure 4). FRO4 also upregulated when exposed to 24 hours of z3HAC alone with a 1.3-fold increase compared to control expression levels (P=0.04: Figure 4). Furthermore, expression levels 24 hours after z3HAC+*S.exigua* OS application were high relative to levels 24 hours after *S. exigua* OS application alone (P=0.02: Figure 4), indicating a priming effect from the combination of volatile exposure and OS resulting in the increase FRO4 expression. Expression levels dropped overall after 6 hours for each treatment when compared to those after 1 and 24 hours, possibly due to the diurnal cycle of plants (Figure 4).

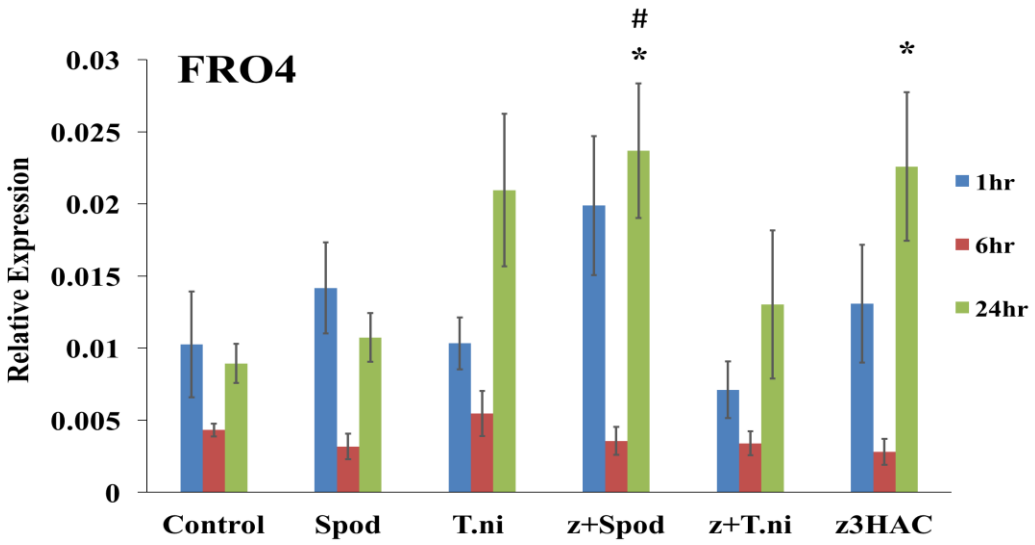

Figure 4. Ferric Reduction Oxidase 4 (FRO4) relative expression levels following exposure to *cis*-3-hexenyl acetate (z3HAC), *Trichoplusia ni* oral secretions *(*T.ni), *Spodoptera exigua* oral secretions (Spod), *cis*-3-hexenyl acetate with subsequent *Spodoptera exigua* oral secretions (z+Spod), and *cis*-3-hexenyl acetate with subsequent *Trichoplusia ni* oral secretions (z+T.ni) relative to control with no oral secretion application or z3HAC exposure. Expression levels were recorded for each treatment at 1-hour (blue) 6-hour (red) and 24-hour (green) time points post treatment application. An asterisk (*) indicates that expression levels were significantly different than that of control at that time point, as determined by paired t-tests. A number sign (#) indicates significantly increased expression with *cis*-3-hexenyl acetate prior to oral secretions relative to expression under oral secretions alone, as determined by paired t-tests.

FRO6 was activated after 24 hours of z3HAC exposure. FRO6 was primed by the combination of z3HAC+*S. exigua* OS 24 hours post treatment application.

FRO6 did not experience increased expression under any treatment at the 1 or 6-hour time point (Figure 5). Expression of FRO6 dropped to almost non-existent levels after 6 hours of each treatment and rose again after 24 hours, again possibly due to the diurnal cycle of plants (Figure 5). Rising after 24 hours, FRO6 expression significantly increased under z3HAC exposure relative to control levels (P=0.03; Figure 5). Furthermore, expression levels 24 hours after z3HAC+*S. exigua* OS application were high relative to levels 24 hours after *S. exigua* OS application alone (P=0.04), indicating a priming effect from the combination of z3HAC exposure and OS application resulting in the increased expression of FRO6 (Figure 5).

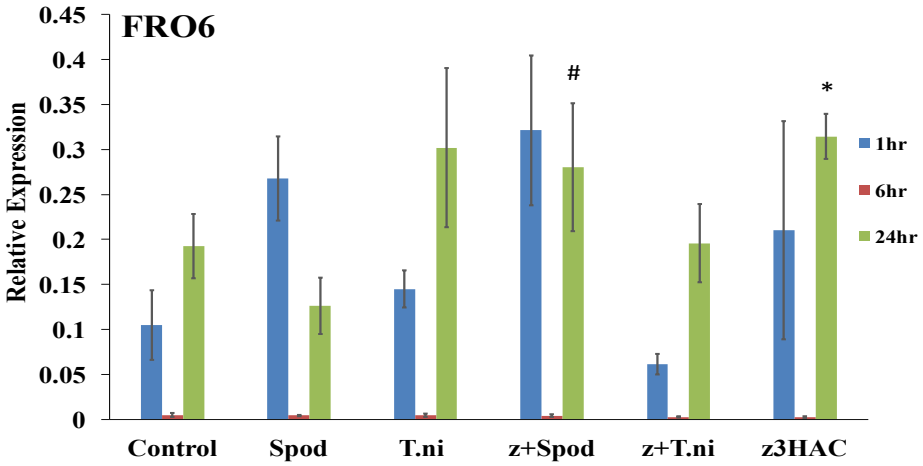

Figure 5. Ferric Reduction Oxidase 6 (FRO6) relative expression levels following exposure to *cis*-3-hexenyl acetate (z3HAC), *Trichoplusia ni* oral secretions (T.ni), *Spodoptera exigua* oral secretions (Spod), *cis*-3-hexenyl acetate with subsequent *Spodoptera exigua* oral secretions (z+Spod), and *cis*-3-hexenyl acetate with subsequent *Trichoplusia ni* oral secretions (z+T.ni) relative to control with no oral secretion application or z3HAC exposure. Expression levels were recorded for each treatment at 1-hour (blue) 6-hour (red) and 24-hour (green) time points post treatment application. An asterisk (*) indicates that expression levels were significantly different than that of control at that time point, as determined by paired t-tests. A number sign (#) indicates significantly increased expression due to with *cis*-3-hexenyl acetate prior to oral secretions relative to expression under oral secretions alone, as determined by paired t

FRO7 was activated after 1 hour of z3HAC+*S. exigua* exposure.

Out of all of the ferric reduction oxidase genes, FRO7 had the highest relative expression levels overall (Figure 6). FRO7 under z3HAC ($\bar{x}$=2.80) at the 24-hour time point had the highest relative expression of all of the FROs in this study (Figure 6). Even though expression levels were high overall for FRO7 at all time-points, expression of FRO7 only significantly increased 1 hour after z3HAC+*S. exigua* OS application with a 2-fold upregulation (P=0.03; Figure 6). Similar to FRO6, expression dropped to nearly non-existent levels after 6 hours of each treatment and rose again after 24 hours, possibly due to the diurnal cycle of plants. No significant priming of FRO7 by z3HAC took place under any treatments at any time points.

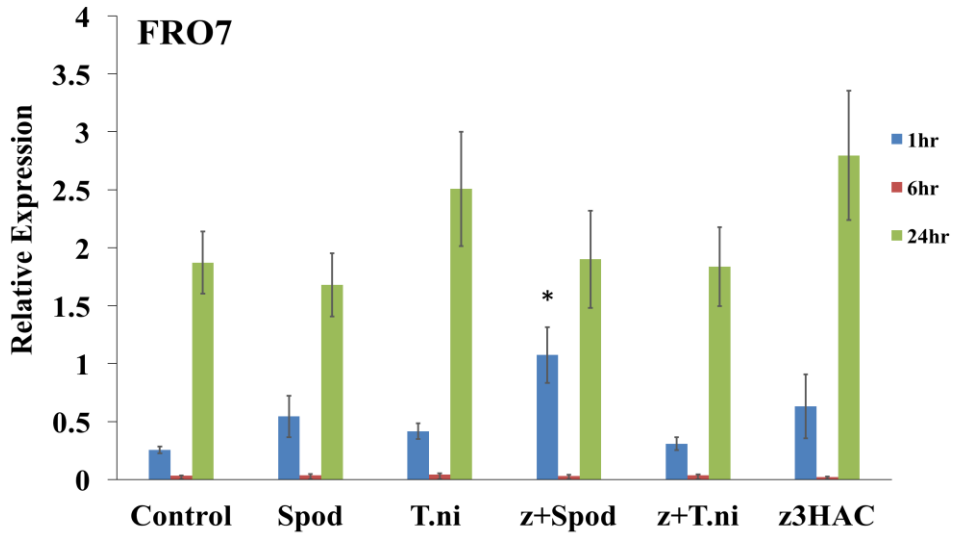

Figure 6. Ferric Reduction Oxidase 7 (FRO7) relative expression levels following exposure to *cis*-3-hexenyl acetate (z3HAC), *Trichoplusia ni* oral secretions *(*T.ni), *Spodoptera exigua* oral secretions (Spod), *cis*-3-hexenyl acetate with subsequent *Spodoptera exigua* oral secretions (z+Spod), and *cis*-3-hexenyl acetate with subsequent *Trichoplusia ni* oral secretions (z+T.ni) relative to control with no oral secretion application or z3HAC exposure. Expression levels were recorded for each treatment at 1-hour (blue) 6-hour (red) and 24-hour (green) time points post treatment application. An asterisk (*) indicates that expression levels were significantly different than that of control at that time point, as determined by paired t-tests. A number sign (#) indicates significantly increased expression with *cis*-3-hexenyl acetate prior to oral secretions relative to expression under oral secretions alone, as determined by paired t-tests.

FRO8 is not activated under any treatment at any time point.

Expression levels of the Ferric Reduction Oxidase 8 gene were high overall relative to FRO4, FRO5, and FRO6 with overall exression falling just short of that of FRO7 (Figure 8). However, expression levels of FRO8 were not significantly upregulated under any treatments at any time point and FRO8 did not experience any significant priming effect.

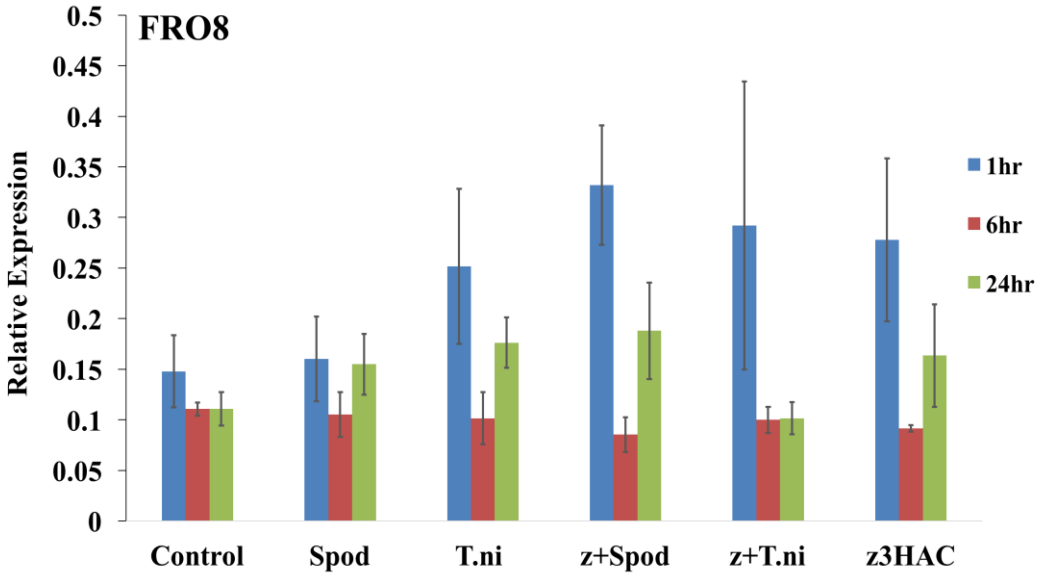

Figure 7. Ferric Reduction Oxidase 8 (FRO8) relative expression levels following exposure to *cis*-3-hexenyl acetate (z3HAC), *Trichoplusia ni* oral secretions *(*T.ni), *Spodoptera exigua* oral secretions (Spod), *cis*-3-hexenyl acetate with subsequent *Spodoptera exigua* oral secretions (z+Spod), and *cis*-3-hexenyl acetate with subsequent *Trichoplusia ni* oral secretions (z+T.ni) relative to control with no oral secretion application or z3HAC exposure. Expression levels were recorded for each treatment at 1-hour (blue) 6-hour (red) and 24-hour (green) time points post treatment application. An asterisk (*) indicates that expression levels were significantly different than that of control at that time point, as determined by paired t-tests. A number sign (#) indicates significantly increased expression with *cis*-3-hexenyl acetate prior to oral secretions relative to expression under oral secretions alone, as determined by paired t-tests.

Discussion

The specific objective of this study was to measure transcriptional responses of FROs to herbivore oral secretions (OS) and plant-derived volatile cues. Results from this study show that FROs do differentially increase expression levels in response to herbivory and volatile exposure. Specifically, the exposure to GLV z3HAC alone induced increased expression of FRO3, FRO4, and FRO6. The exposure to z3HAC plus subsequent application of *S. exigua* OS induced increased expression of FRO3, FRO4, and FRO7. Increased expression of FRO3 was also induced by z3HAC exposure plus subsequent *Trichoplusia* OS. In addition, expression of FRO4 and FRO6 was primed by the combination of z3HAC and *Spodoptera exigua* OS after 24 hours of exposure.

According to these results, FRO7 and FRO8 have the highest relative expression in the leaves of *A. thaliana*. These findings are consistent with other recent work showing FRO7 localized to chloroplasts and FRO8 localized to leaf veins (Wu et al. 2005; Jain et al. 2008). The chloroplast is a major iron sink within a leaf and significantly increased expression levels of FRO7 following z3HAC+*S. exigua* OS indicates FRO7 responds directly to herbivory, possibly to maintain iron homeostasis in the face of herbivory (Guerinot and Yi 1994). The overall high relative expression with insignificant upregulation of FRO8 is consistent with expression profiles of FRO8 showing FRO8 as expressed at constitutively high levels in leaf veins (Wu et al. 2005).

Expression profiling carried out by Wu et al. in 2005 indicates FRO4 has the lowest expression levels in the metalloreductase gene family. This study's findings are congruent with this profile because FRO4 showed the lowest relative expression levels overall. However, FRO4 did significantly increase expression activity 24 hours following z3HAC exposure, suggesting perception of HIPV by FRO4. While at a relatively low level, FRO4's significant response to

z3HAC exposure suggests a direct response to herbivory. FRO4 also experienced a priming effect by the combination of z3HAC and *Spodoptera exigua* OS, suggesting iron uptake and homeostasis in leaves may be important in plant anti-herbivore defense (Frost et al. 2008). Similar to FRO4, FRO6 increased expression induced by z3HAC exposure as well as priming from the combination of z3HAzC and *Spodoptera exigua* OS further reinforces the possibility that FROs respond to herbivory and play a biological role in plant anti-herbivore response (Frost et al. 2008). Due to a plant diurnal cycle and this study's 12:12 light: dark cycle, the down regulation of FRO6 expression at the 6-hour time point is congruent with results of previous studies that indicate FRO6 as light-dependent (Feng et al. 2006).

FRO3 increases expression levels to maintain iron homeostasis under iron-deficient conditions in the roots of *A. thaliana* (Jain et al. 2014). However, FRO3 has also been identified as localized in mitochondrial membranes with non-overlapping expression patterns as FRO8 (Wu et al. 2005; Jain and Connolly 2013). Similar with results of Jain and Connolly, this study does indicate FRO3 is expressed in *A. thaliana* leaves with a significant increase 24 hours after exposure alone. This induced expression in response to a combination of herbivory and volatile exposure shows FRO3 as directly responsive to herbivory or the perception thereof.

With the objective of measuring transcriptional activation of FROs in response to a combination of herbivory and GLV z3HAC exposure, this study shows that FROs do respond to herbivory and HIPV perception with differentially increased expression. Induced expression in response to herbivory and HIPV exposure suggests that FROs may play a biological role in plant anti-herbivore response. Whereas a recent study indicates activation of below ground FROs in response to below ground volatiles released from root colonization of *Trichoderma* fungi (Martinez-Medina et al. 2017), this study shows activation of above ground FROs in response to

above ground volatiles released upon herbivory. Because this is the first study to link ferric reduction oxidases and herbivory, future work should seek to identify a mechanistic link between iron homeostasis and plant defense. With iron as a necessary element for plants to carry out essential metabolic functions, the role of FROs may be essential to stabilizing a plant during herbivore response. Further investigation could also include looking at promoter regions for activation sites as well as considering the possibility of FRO activation triggered by metabolites known to regulate plant defenses such as jasmonic acid (Creelman 1995).

Acknowledgements

I would like to give my thanks and gratitude Dr. Christopher Frost for the never wavering guidance, support, and enthusiasm he has given me throughout the completion of this project. I would like to thank Dr. Leila Pazouki, a postdoctoral researcher in the Frost Lab at the University of Louisville, for the endless lab hours she spent teaching me necessary techniques and pouring through data. I would like to thank my fellow lab members, Sarah Bissmeyer, Grace Freudlich, and Abhinav Maurya for providing a lab environment filled with the desire learn and room to grow. I would also like to thank Dr. Eugene Mueller and Dr. Mark Running for taking the time to participate as members of the committee for this Senior Honors Thesis. Lastly, I would like to thank the University of Louisville, without which this opportunity would never have been possible.

,

References

Ainhoa Martínez-Medina, Saskia C.M. Van Wees and Corné M.J. Pieterse. (2017). Airborne Signals from *Trichoderma* Fungi Stimulate Iron Uptake Responses in Roots Resulting in Priming of Jasmonic Acid-Dependent Defenses in Shoots of *Arabidopsis thaliana* and *Solanum lycopercum. Plant, Cell, and Environment* (2017).

Andrew Dancis, Dragos G. Roman, Gregory J. Anderson, Alan G Hinnebusch and Richard D. Klausner. (1992). Ferric Reductase of Saccharomyces cerevisiae: Molecular Characterization, Role in Iron Uptake, and Transcriptional Control by Iron. *Proceedings of the National Academy of Sciences of the United States of America,* Vol. 89, No. 9 (May 1, 1992). 3869-3873

Brian M. Waters, Dale G. Blevins and David J. Eide. (2002). Characterization of FRO1, a Pea Ferric-Chelate Reductase Involved in Root Iron Acquisition. *Plant Physiology,* Vol. 129 No. 1 (May 2002) 85-94.

Chang, S., Puryear, J., and Cairney. 1993. A simple and efficient method for isolating RNA from

Chang Yan Li, Wen-Yan Li, Hai Miao, Shuai-Qi Yang, Ri Li Xiang, WangWen-Qiang, Li Kun-Ming Chen. (2016). Comprehensive Genomic Analysis and Expression Profiling of the NOX Gene Families under Abiotic Stresses and Hormones in Plants. *Genome Biology and Evolution,* Vol. 8 No. 3 (March 2016) 791-810.

pine trees. *Plant Molecular Biology Reporter* 11(2):113-116

Choudhary DK, Prakash A, Johri BN. Induced systemic resistance (ISR) in plants: mechanism of action. Indian J Med Microbiol. 2007;47:289–297.

Clara K Cohen, Wendell A. Norvell and Leon V. Kochian. (1997). Induction of the Root Cell Plasma Membrane Ferric Reductase: An Exclusive Role for Fe and Cu. *Plant Physiology,* Vol. 114 No. 3 (July 1997) 1061-1069

Creelman R. A., J. E. Mullet. (1995). Jasmonic Acid Distribution and Action in Plants: Regulation During Development and Response To Biotic and Abiotic Stress. *Proc. Natl. Acad. Sci. USA.* 1995 May 9. 1995 May 9; 92(10): 4114–4119.

Dancis A,. Dragos G. Roman, Gregory J. Anderson, Alan G Hinnebusch and Richard D. Klausner. (1992). Ferric Reductase of Saccharomyces cerevisiae: Molecular Characterization, Role in Iron Uptake, and Transcriptional Control by Iron. *Proceedings of the National Academy of Sciences of the United States of America,* Vol. 89, No. 9 (May 1, 1992). 3869-3873

Dong F., Fu X., Watanabe N., Su X., Yan Z. (2015). Recent Advances in the Emissions and Functions of Plant Vegetative Volatiles. *Molecules.* 21(2): 124

Dubiella U. et al. 2013. Caldium-dependent protein kinase/NADPH oxidase activation circuit is required for rapid defense signal propagation. Proc Natl Acad Sci USA, 110:8744-8749

Frost CJ, Heidi M. Appel, John E. Carlson, Consuelo M. De Moreas, Mark C. Mescher, Jack C. Shultz. (2007). Within-plant signaling via volatiles overcomes vascular constraints on systemic signaling and primes responses against herbivores. *Ecology Letters.* 2007. 10(6): 490-498.

Frost CJ, Mark C. Mesher. Christopher Dervinis, John M. Davis, John E. Carlson, Consuelo M. De Moreas. 2008. Priming defense genes and metabolites in hybrid poplar by green leaf volatile cis-3-hexanyl acetate. *New Phytologist.* 2008 Nov; 180(3): 722-734

Frost CJ, Mark C. Mesher, John E. Carlson, Consuelo M. De Moreas. (2008). Plant Defense Priming against Herbivores: Getting Ready for a Different Battle. *Plant Physiology.* 2008 Mar; 146(3): 818–824.

Frost CJ, Nyamdari B, Tsai C-J, Harding SA (2012) The Tonoplast-Localized Sucrose Transporter in *Populus* (PtaSUT4) Regulates Whole-Plant Water Relations, Responses to Water Stress, and Photosynthesis. PLoS ONE7(8): e44467. https://doi.org/10.1371/journal.pone.0044467

Guerinot ML, Yi Y (1994) Iron: Nutritious, Noxious, and Not Readily Available. *Plant Physiology,* Vol. 104, No. 3 (March 1994). 815-820.

Guerinot ML, Kim SA (2007). Mining Iron: Iron Uptake and Transport and Plants. NCBI. May 25;581(12):2273-80

Guosheng Liu, David L. Greenshields, Ramaswami Sammynaiken, Rozina N. Hirii, Gopalan Selyarai and Yangdou Wei. (2007). Targeted Alterations in Iron Homeostasis Underlie Plant Defenes Responses. *Journal of Cell Science,* Vol. 120 (2007) 596-605.

Haizhong Feng, Fengying An, Suzhi Zhang, Zhengdong Ji, Hong-Qing Ling and Jianru Zuo. (2006). Light Regulated, Tissue Specific, and Cell Differentiation-Specific Expression of the Arabidopsis Fe (III)-Chelate Reductase Gene AtFRO6. *Plant Physiology,* Vol. 140, No. 2 (April 2006). 1345-1354.

Hulian Wu, Lihua Li, Juan Du, Youxi Yuan, Xudong Cheng and Hong-Qing Ling. (2005). Molecular and Biochemical Characterization of the Fe(III) Chelate Reducase Gene Family in *Arabidopsis thaliana. Plant and Cell Physiology,* Vol. 46 No. 9 (September 2005) 1505-1514.

Jain A., Connollu E. L. (2013). Mitochondrial iron transport and homeostasis in plants. *Front. Plant Sci.* 4:34(2013).

Jain, Anshika. Grandon T. Wilson. Erin L. Connolly. (2014). The Diverse Roles of FRO family metalloreductases in Iron and Copper Homeostasis. *Frontiers in Plant Science* Vol. 5 No. 100 (2014)

Jeeyon Jeong, Christopher Cohu, Loubna Kerkeb, Marinus Pilon, Erin L. Connolly and Mary Lou Guerinot. (2008). Chloroplast Chelate Reductase Activity is Essential for Seedling Viability under Iron-Limiting Conditions. *Proceedings of the National Academy of Sciences of the United States of America,* Vol. 105. No. 30 (July 2008). 10619-10624.

Kieu N.P., Aznar A., Segond D., Rigault N., Simond-Cote E., Kunz C., Dellagi A. (2012). Iron deficiency affects plant defense responses and confers resistance to *Dickeya dandantii* and *Botrytis cinerea. Molecular Plant Pathology.* 13, 816-827.

Li W. et al. 2009. Phylogenetic analysis, structural evolution and functional divergence of the 12-oxophytodienoate acid reductase gene family in plants. BMC Evolutionary Biology 9:90

Martinez-Medina Ainhoa, Saskia C.M. Van Wees, & Corne M.J. Pieterse. 2017. Airborne signals from Trichoderma fungi stimulate iron uptake responses in roots resulting in priming of jasmonic aciddependent defences in shoots of Arabidopsis thaliana and Solanum lycopersicum. *Plant, Cell, & Environment,* 2017 Nov;40(11):2691-2705.

Marscher H (1995) Mineral Nutrition of Higher Plants. Academic Press, San Diego

Mary Lou Guerinot and Ying Yi. (1994). Iron: Nutritious, Noxious, and Not Readily Available. *Plant Physiology,* Vol. 104, No. 3 (March 1994). 815-820.

Nam Phuong Kieu, Aude Aznar, Deigo Segond, Martine Rigault, Elizabeth Simond-Cote, Caroline Kunz, Marie Christine Soulie, Dominique Expert and Alia Dellagi. (2012). Iron Deficiency Affects Plant Defense Responses and confers resistance to *Dickeya dadantii* and *Boytrytis cinerea. Molecular Plant Pathology,* Vol. 13 No. 8 (October 2012) 816-827.

Nigel J. Robinson, Catherine M. Procter, Erin L. Connolly and Mary Lou Guerinot. (1999). A Ferric-Chelate Reductase For Iron Uptake from the Soils. *Nature,* Vo. 397 (February 1999) 694-697.

Oliver Thimm, Bernd Essigmann, Sebastian Kloska, Thomas Altmann and Thomas J. Buckhout. (2001). Response of Arabidopsis to Iron Deficiency Stress as Revealed by Microarray Analysis. *Plant Physiology.* Vol. 127 No. 3 (November 2001) 1030.

Rodriguez-Saona CR , LE Rodriguez-Saona, and Frost CJ. 2009. Herbivore-induced volatiles in the perennial shrub, Vaccinium corymbosum, and their role in inter-branch signaling. Journal of Chemical Ecology 35(2): 163-175

Shujun Chang, Jeff Puryear and John Cairney. (1993). A Simple and Efficient Method for Isolating RNA From Pine Trees. *Plant Molecular Biology Reporter,* Vol. 11. No. 2 (1993) 113-116.

The North American Arabidopsis Steering Committee. (2017). *TAIR.* http://www.arabidopsis.org/index.jsp.

War A. Rashid, Hari Chand Sharma, Michael G. Paulraj, Mohd Yousf War, Savarimuthu Ignacmuthu (2011). Herbivore Induced Plant Volatiles. Their Role in Plant Defense for Pest Management. *Plant Signaling and Behavior,* 2011 Dec 1; 6(12): 1973-1978)

Wu H., Lihua Li, Juan Du, Youxi Yuan, Xudong Cheng and Hong-Qing Ling. (2005). Molecular and Biochemical Characterization of the Fe(III) Chelate Reducase Gene Family in *Arabidopsis thaliana. Plant and Cell Physiology,* Vol. 46 No. 9 (September 2005) 1505-1514.

Appendix

Supplementary Figure I

Supplementary Figure II

Supplementary Figure III

Supplementary Figure IV

Supplementary Figure V

Supplementary Figure I

(A)

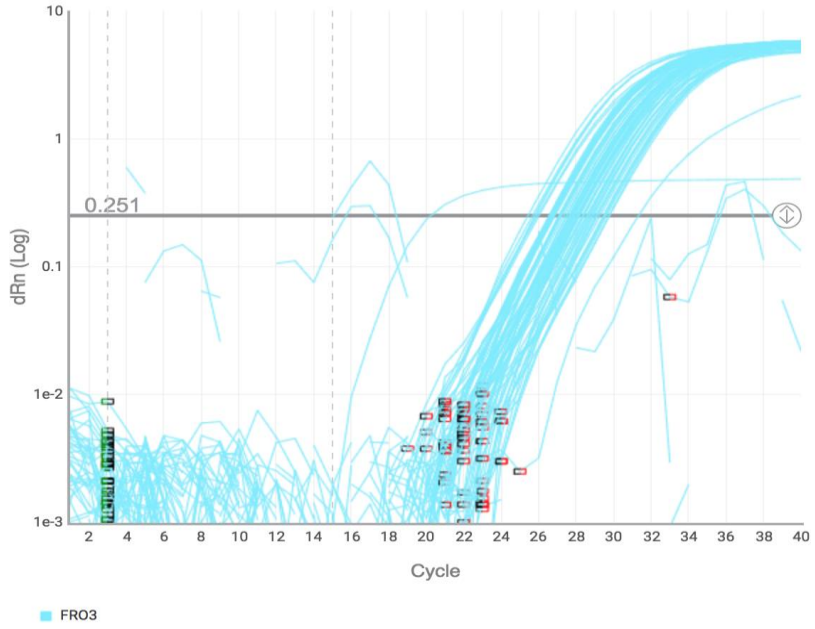

(B)

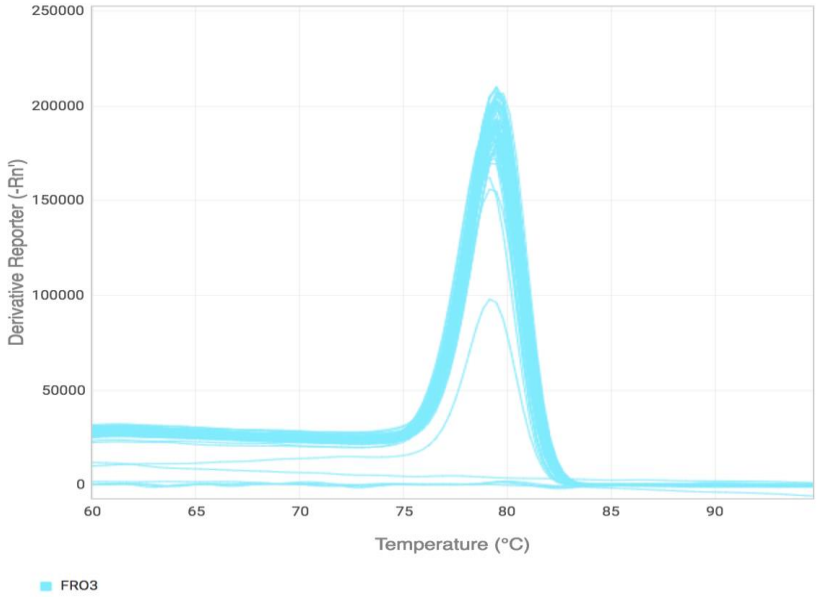

Supplementary Figure I. Real-time qPCR results of FRO3 for all 6-hour FRO3 samples. Amplification plot (A) shows accumulation of PCR product (FRO3) from cycle to cycle with the cycle threshold (Ct) values ranging from 26.01 and 29.7. All samples were in exponential growth at 0.251 dRn(Log). The melting curve (B) indicates a pure, single amplicon from FRO3 qPCR. Both amplification plot and melting curve were generated on ThermoFisher Scientific.

Supplementary Figure II

(A)

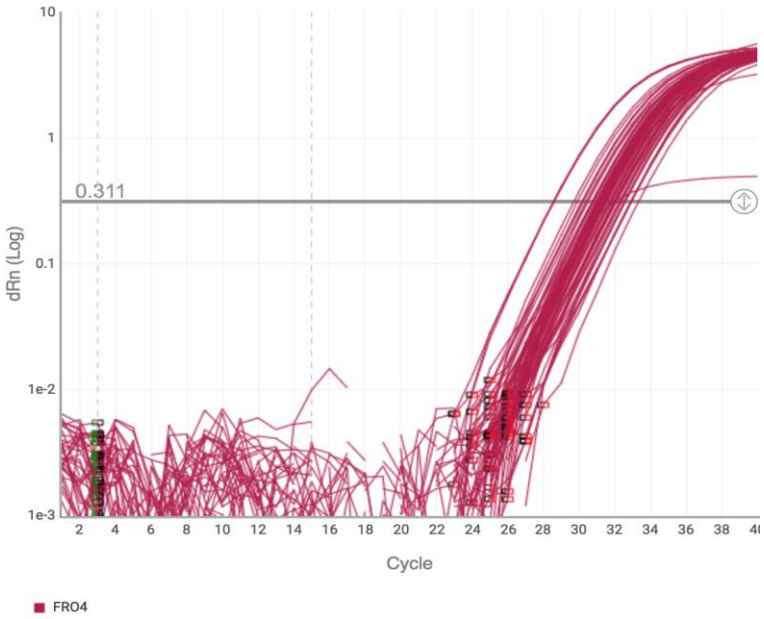

(B)

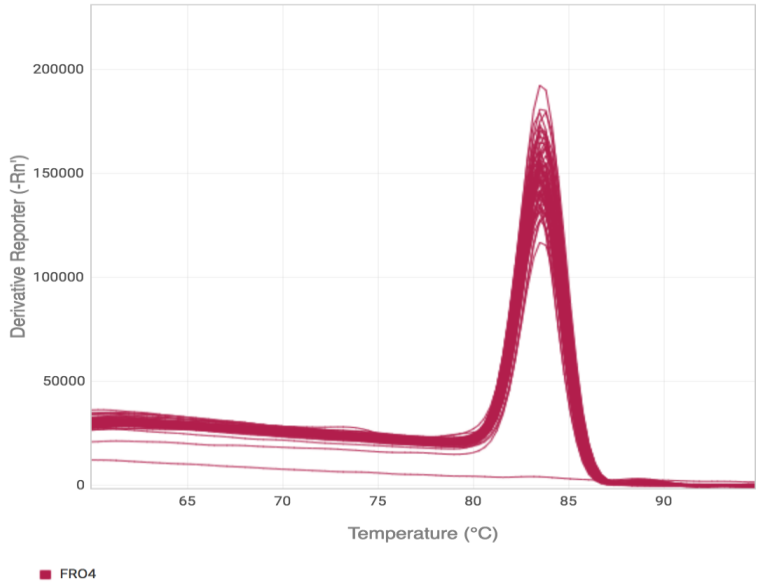

Supplementary Figure II. Real-time qPCR results of FRO4 for all 6-hour FRO4 samples. Amplification plot (A) shows accumulation of PCR product (FRO4) from cycle to cycle with the cycle threshold (Ct) values ranging from 28.59 and 32.92. All samples were in exponential growth at 0.311 dRn(Log). The melting curve (B) indicates a pure, single amplicon from FRO3 qPCR. Both amplification plot and melting curve were generated on ThermoFisher Scientific.

Supplementary Figure III

(A)

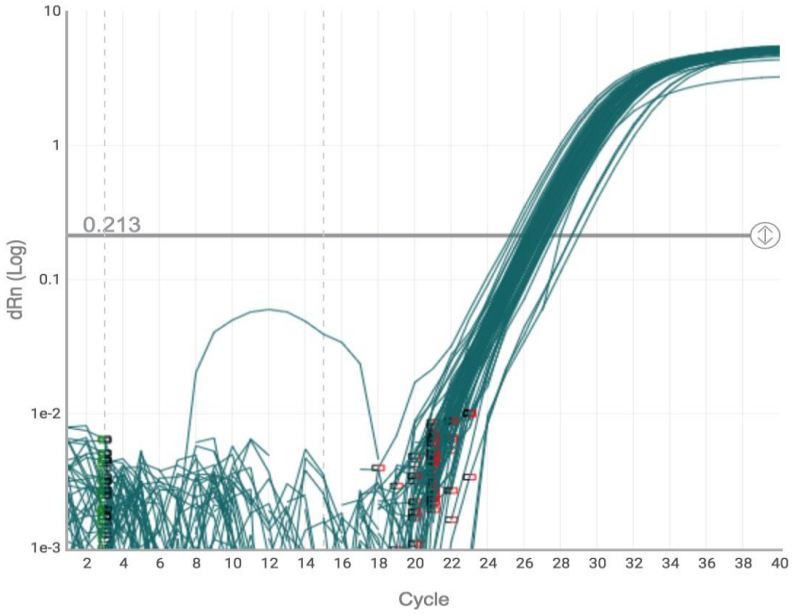

(B)

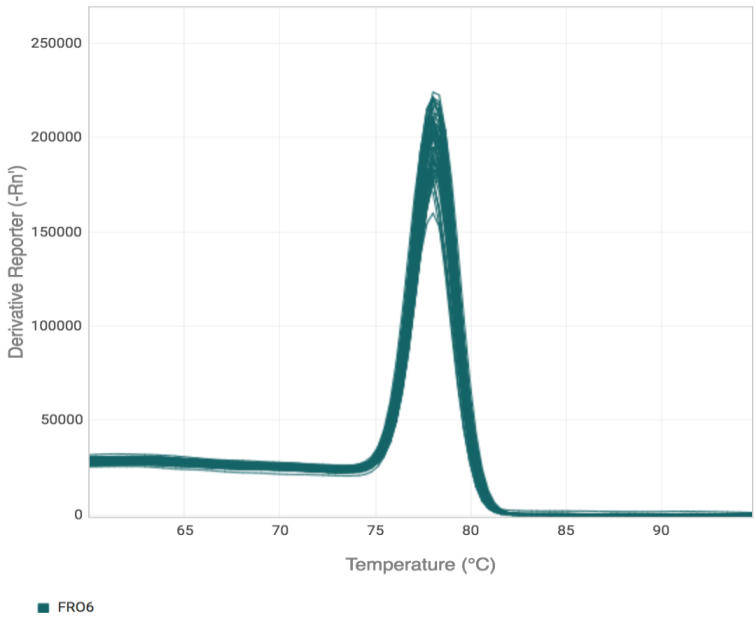

Supplementary Figure III. Real-time qPCR results of FRO6 for all 6-hour FRO6 samples. Amplification plot (a) shows accumulation of PCR product (FRO6) from cycle to cycle with the cycle threshold (Ct) values ranging from 25.09 and 36.32. All samples were in exponential growth at 0.311 dRn(Log). The melting curve (b) indicates a pure, single amplicon from FRO6 qPCR. Both amplification plot and melting curve were generated on ThermoFisher Scientific.

Supplementary Figure IV

(A)

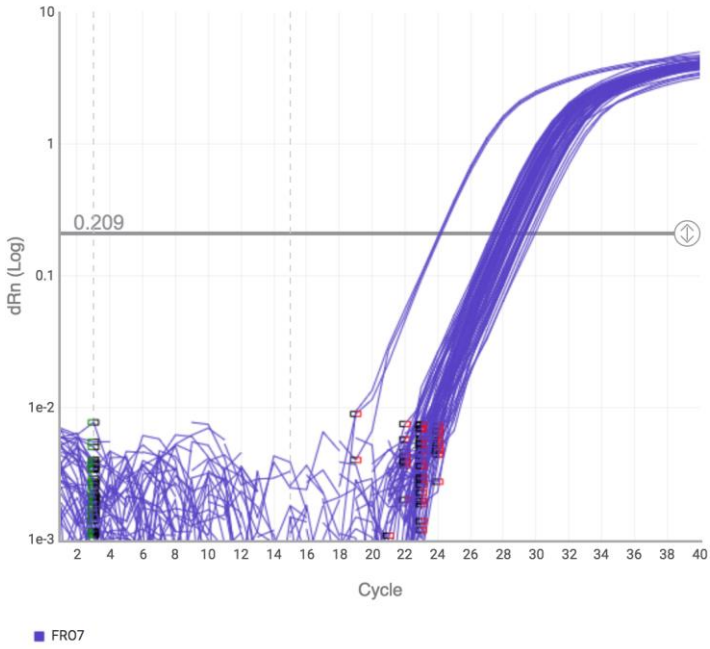

(B)

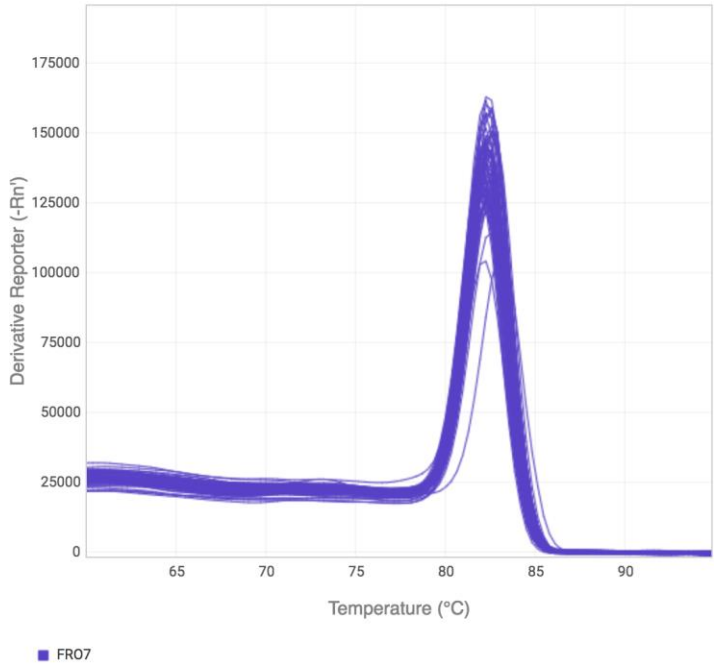

Supplementary Figure IV. Real-time qPCR results of FRO7 for all 6-hour FRO7 samples. Amplification plot (a) shows accumulation of PCR product (FRO7) from cycle to cycle with the cycle threshold (Ct) values ranging from 22.21 and 30.02. All samples were in exponential growth at 0.311 dRn(Log). The melting curve (b) indicates a pure, single amplicon from FRO6 qPCR. Both amplification plot and melting curve were generated on ThermoFisher Scientific.

Supplemental Figure V

(A)

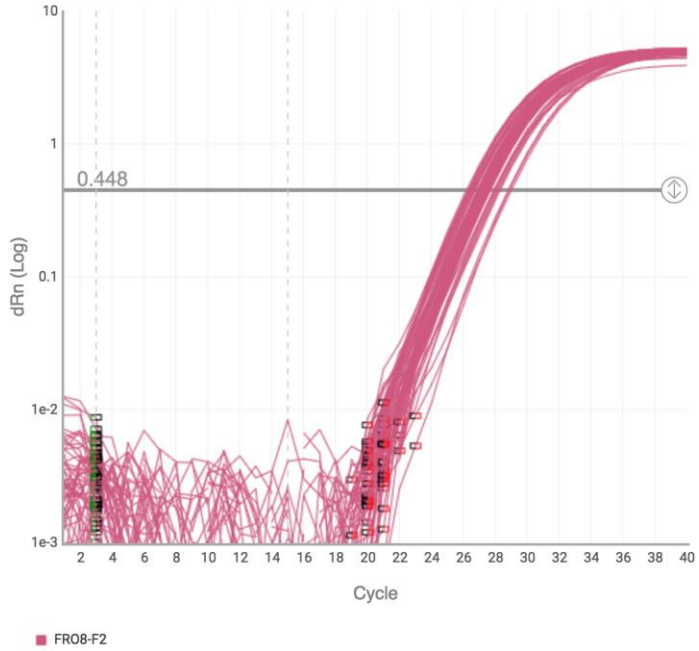

(B)

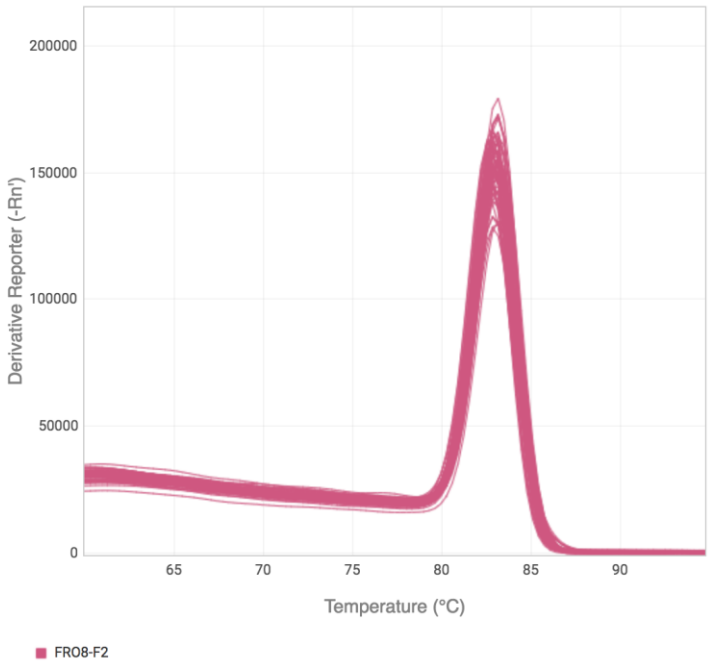

Supplementary Figure V. Real-time qPCR results of FRO8 for all 6-hour FRO8 samples. Amplification plot (a) shows accumulation of PCR product (FRO8) from cycle to cycle with the cycle threshold (Ct) values ranging from 27.67 and 32.62. All samples were in exponential growth at 0.311 dRn(Log). The melting curve (b) indicates a pure, single amplicon from FRO6 qPCR. Both amplification plot and melting curve were generated on ThermoFisher Scientific.